Molecular imaging with seeded and SASE XFEL illumination

Harry Quiney
ARC Centre for Coherent X-ray Science
School of Physics
The University of Melbourne

Workshop on XFEL Seeding, 19-20 July 2012, Hamburg, Germany

Acknowledgements

The Centre of Excellence for Coherent X-ray Science is funded by the Australian Research Council

- Keith Nugent, Andrew Peele, Brian Abbey, Ruben Dilanian, Victor Streltsov, Andrew Martin, David Vine, Bo Chen, Sam Flewett, Lachlan Whitehead, Rebecca Ryan, Evan Curwood, Angela Torrance, Clare Henderson, Isaac Peterson, Corey Putkunz (Melbourne)

- Garth Williams (SLAC)

- Ian McNulty (APS Argonne)

Overview

Connections between electronic processes, structural disorder and partially coherent diffractive imaging.

- Imaging of single biomolecules using XFEL sources
- Electronic damage and partial coherence
- Imaging of biomolecular nanocrystals using XFEL sources
- Structural disorder in nanocrystals and partial coherence
- Radiation-induced changes in C_{60}

Seeded XFEL sources: motivation

Production of transform-limited X-ray pulses through self-seeding at the Eurpoean XFEL, Geloni, Kocharyan and Saldin, DESY preprint (2012).

"Combination of self-seeding and a tapering undulator would be of great importance for atomic resolution imaging of single macromolecules".

Projected transform-limited source characteristics:

- 2×10^{12} photons per pulse
- 7 fs FWHM pulse duration
- 1.5 Å wavelength
- "full" spatial coherence ($\sigma_L > 1 \times 10^{-6}$m).

Seeded XFEL sources: motivation

Any advantage that a seed source might have over a SASE source in imaging applications will fall into one of two general categories

1. The characteristics of the source render the experiment closer to "the ideal model": phase retrieval of an exit surface wave using coherent diffractive imaging, with subsequent modelling to construct a ground-state molecular electron density.

2. The statistical characteristics of the source render the deviations from this ideal model more accessible to analysis in order to extract coherent information (the chemical structure) from partially coherent data (scattering measurements)

We will see that the advantages of seeding are of Type 2.

Seeded XFEL sources: motivation

- The principal distinguishing characteristic of a seeded source over a SASE source is the production of transform-limited pulses $\delta\lambda/\lambda \simeq 10^{-5}$ that are essentially monochromatic and spatially coherent.

- It will also likely be the case that the shot-to-shot variation in these seeded pulses will produce a distribution in peak intensities and central wavelengths whose ensemble average may be represented by smooth distributions around λ_0 and I_0.

- The SASE pulses each have $\delta\lambda/\lambda \simeq 0.01$ and an apparently chaotic intensity profile.

Does the decrease in bandwidth or the transform-limiting of seeded pulses convey any intrinsic advantage over SASE pulses *in imaging applications*?

Imaging with a spectrally broad source

LETTERS
PUBLISHED ONLINE: 26 JUNE 2011 | DOI: 10.1038/NPHOTON.2011.125
nature photonics

Lensless imaging using broadband X-ray sources

Brian Abbey[1], Lachlan W. Whitehead[1], Harry M. Quiney[1], David J. Vine[1], Guido A. Cadenazzi[1], Clare A. Henderson[1], Keith A. Nugent[1]*, Eugeniu Balaur[2], Corey T. Putkunz[2], Andrew G. Peele[2], G. J. Williams[3] and I. McNulty[4]

Abbey *et al.*, *Nature Photonics*, **5**, 420-424 (2011).

Imaging with a spectrally broad synchrotron source

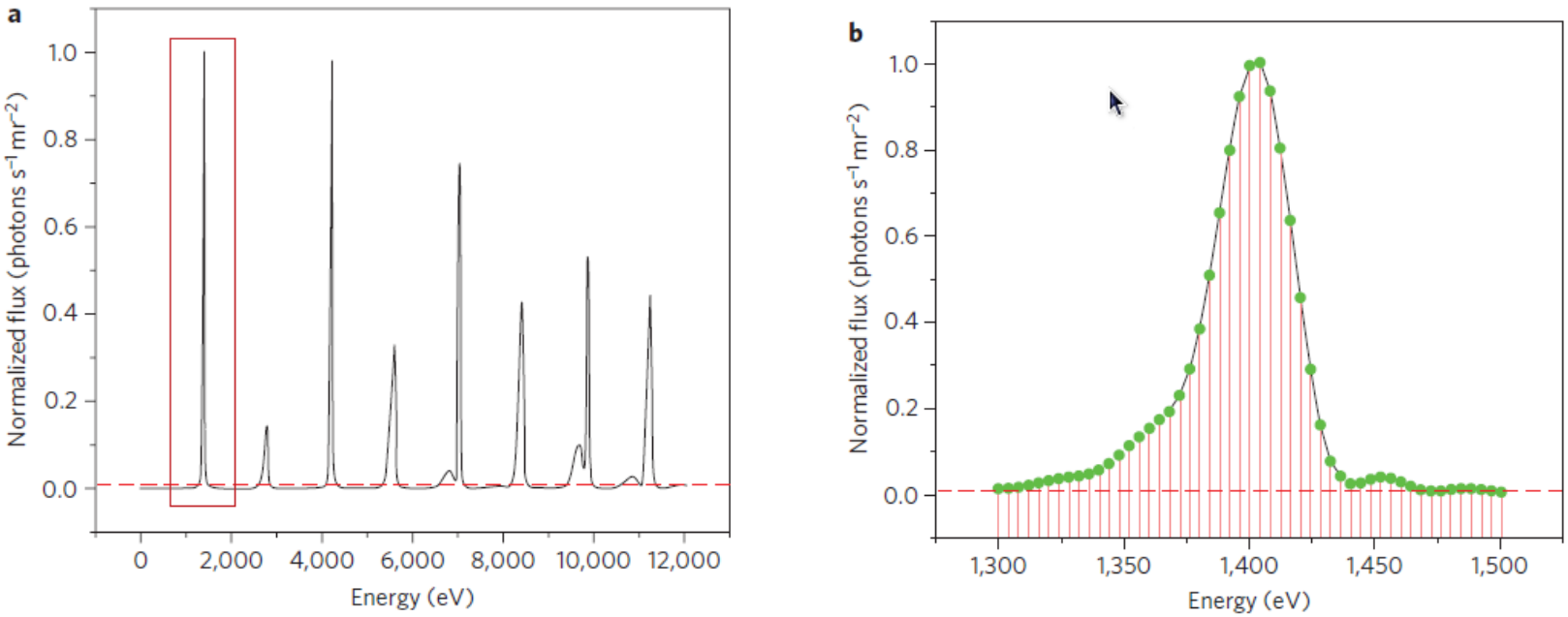

Undulator spectrum (left) and harmonic spectrum (right) at the Advanced Light Source (Chicago). The harmonic is represented by discrete samples in the range 1300 eV- 1500 eV. The frequency grid enables data to be distinguished at the maximum required spatial resolution.

Imaging with a spectrally broad synchrotron source

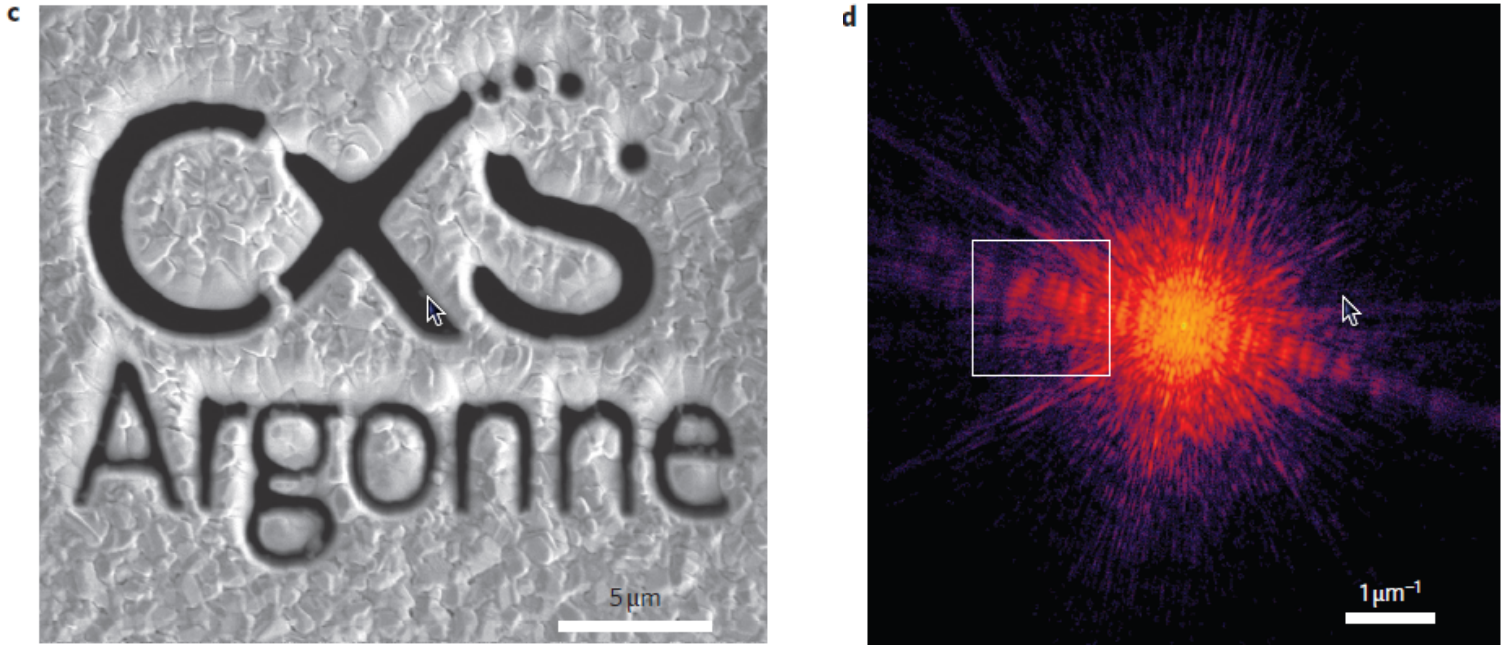

Imaging with a spectrally broad synchrotron source

NATURE PHOTONICS DOI: 10.1038/NPHOTON.2011.125 LETTERS

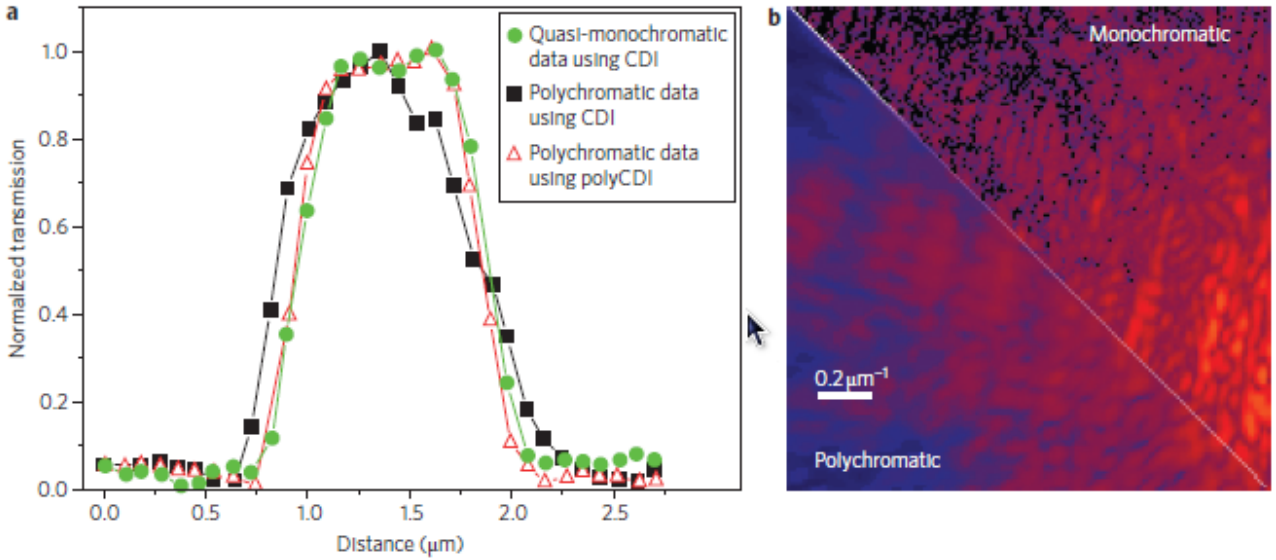

Figure 3 | Comparison of reconstructed image resolution and data. Example resolution lineout comparing the results from Fig. 2a, c and d. The data show that the reconstruction from quasi-monochromatic data (500 × 3 s exposures) gives a virtually identical profile to the polyCDI algorithm reconstruction (500 × 50 ms exposures). The experimentally determined resolutions measured from both sets of data are 150±5 nm. The result obtained from broadband data using just a priori knowledge of the sample to generate the support gives a significantly lower resolution of 320±7 nm. **b**, Comparison of the quasi-monochromatic and broadband data for the region bounded by the white box in Fig. 1d. The polychromatic diffraction pattern is significantly more blurred than the monochromatic equivalent, meaning that it cannot effectively be used to reconstruct the sample ESW without accounting for the spectral distribution.

Spectral width in diffractive imaging

- If we incorporate the spectral distribution in the phase retrieval algorithm, images can be recovered from partially-coherent data essentially *without loss of resolution*: a Type 2 solution.

- Effective limit of bandwidth for partially coherent diffraction is $\delta\lambda/\lambda = 0.08$; SASE pulses already satisfy this condition.

- Projected $\delta\lambda/\lambda$ at 1.5 Å of seeded-tapered European XFEL source is 10^{-5}: monochromatic for imaging purposes.

- The greatest advantage of the seeding procedure is likely to come from control over the distribution of pulses around λ_0 and I_0, rather than narrow bandwidth of any single pulse.

Biomolecular imaging with XFEL

LETTERS
PUBLISHED ONLINE: 19 DECEMBER 2010 | DOI: 10.1038/NPHYS1859
nature physics

Biomolecular imaging and electronic damage using X-ray free-electron lasers

Harry M. Quiney* and Keith A. Nugent

Quiney and Nugent, *Nature Physics*, **7**, 142-146 (2011).

Diffract and destroy imaging

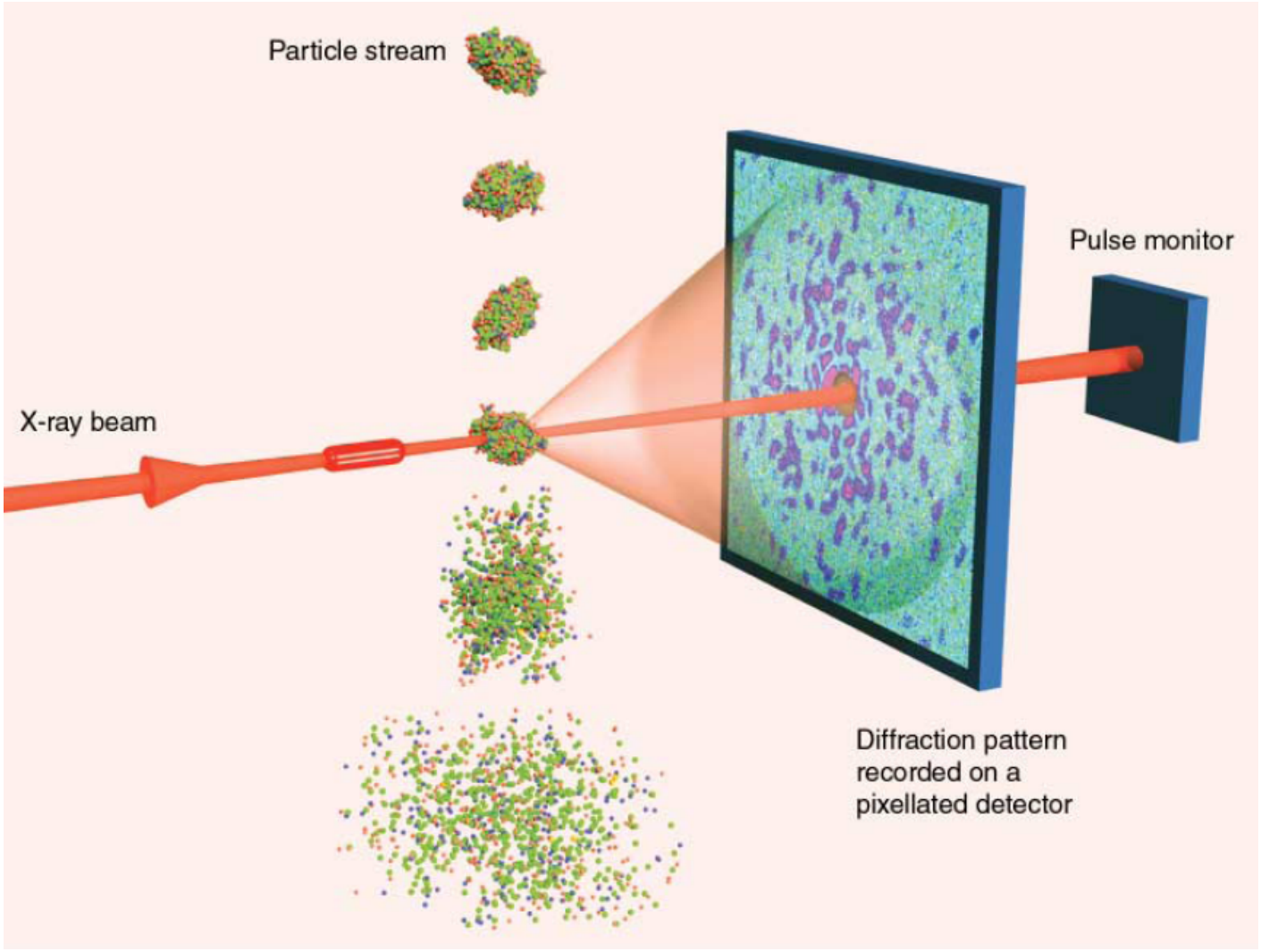

Why the molecule-laser interaction should be short

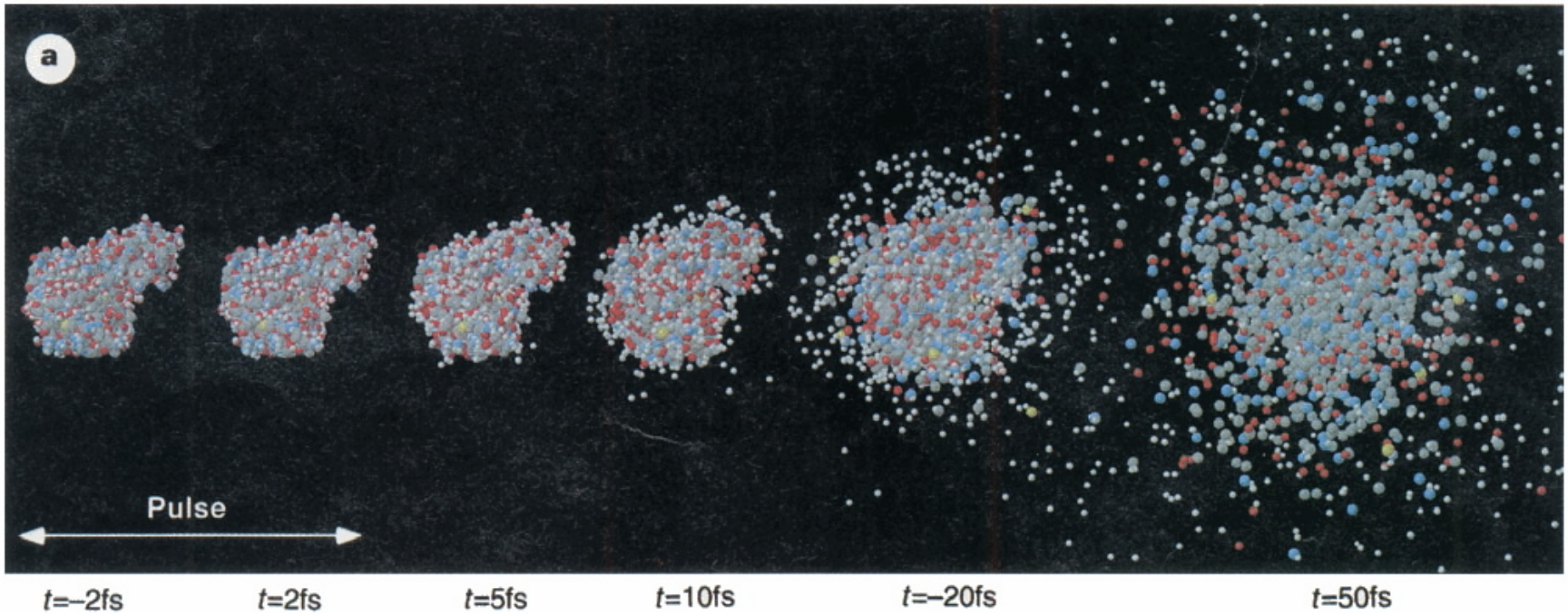

Neutze *et al.*, *Potential for biomolecular imaging with femtosecond X-ray pulses*, Nature, **406**, 752-757 (2000).

Competition between scattering and damage

Electrons, not nuclei, scatter X-rays; a sub-5 fs interaction still involves *very* substantial electronic 'damage' (even for 'frozen' nuclei).

- Dominant high-resolution ('large-q') scattering involves K-shell electrons
- K-shell core-electrons are depleted by X-ray photonionization; 'hollow atoms' are possible.
- K-shell population replenished by Auger process, depleting L-shell.
- Ejected electrons are recaptured by the *huge* positive charge of the residual molecule-ion; further electron impact ionization occurs.
- Breakdown of atomic scattering model; Coulomb explosion.

Electrodynamical approach: *Electrodynamical CDI*

H. M. Quiney and K. A. Nugent, *Nature Physics*, **7** 142-146 (2011).

Assume that scattering probability depends on the instaneous electron density and incident radiation field. The time-dependent molecular form-factor,

$$F_n(\mathbf{q},t) = \sum_Z \sum_{\gamma_Z} \sum_{m_Z} a_n^{Z\gamma_Z m_Z}(t) f^{Z\gamma_Z}(q) \exp(-i\mathbf{q}\cdot\mathbf{R}^Z_{m_Z}),$$

where $a_n^{Z\gamma_Z m_Z}(t)$ is the time-dependent atomic *population* of atomic state function, $|Z,\gamma_Z,m_Z\rangle$, throughout molecule-laser interaction labelled n.

- $|Z,\gamma_Z,m_Z\rangle$ denotes (atomic species,atomic state, atomic instance)

Electrodynamical approach: *Electrodynamical CDI*

Under proposed experimental conditions, photoionization is *ten times* more likely than elastic scattering.

The probability of scattering of a single photon depends on the instantaneous distribution $a_n^{Z\gamma_Z m_Z}(t)$. Two atoms of type Z may be in distinct electronic states, γ_Z and γ'_Z, in measurement n.

The allocation of the populations $a_n^{Z\gamma_Z m_Z}(t)$ is stochastic (depends on n) and will lead to distinct diffraction patterns, typically consisting of (say) 100 photons scattered from molecules that have ejected 1000 photoelectrons.

The number of instantaneous allocations state γ_Z to atom m_Z of type Z to the populations $a_n^{Z\gamma_Z m_Z(t)}$ is *huge*; each is an independent *mode* of an accumulated diffraction dataset.

Electrodynamical approach: *Electrodynamical CDI*

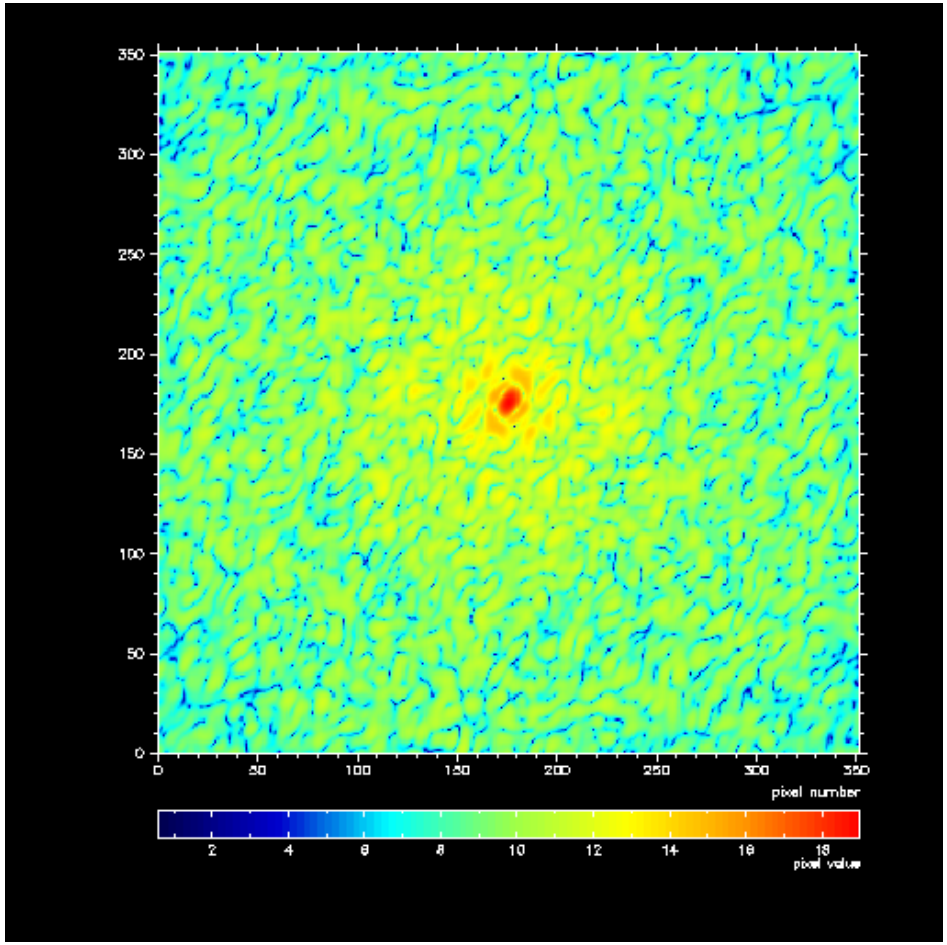

Distributions differing by *ten* randomly-allocated holes (200 frames).

Effect of electronic damage on intensity

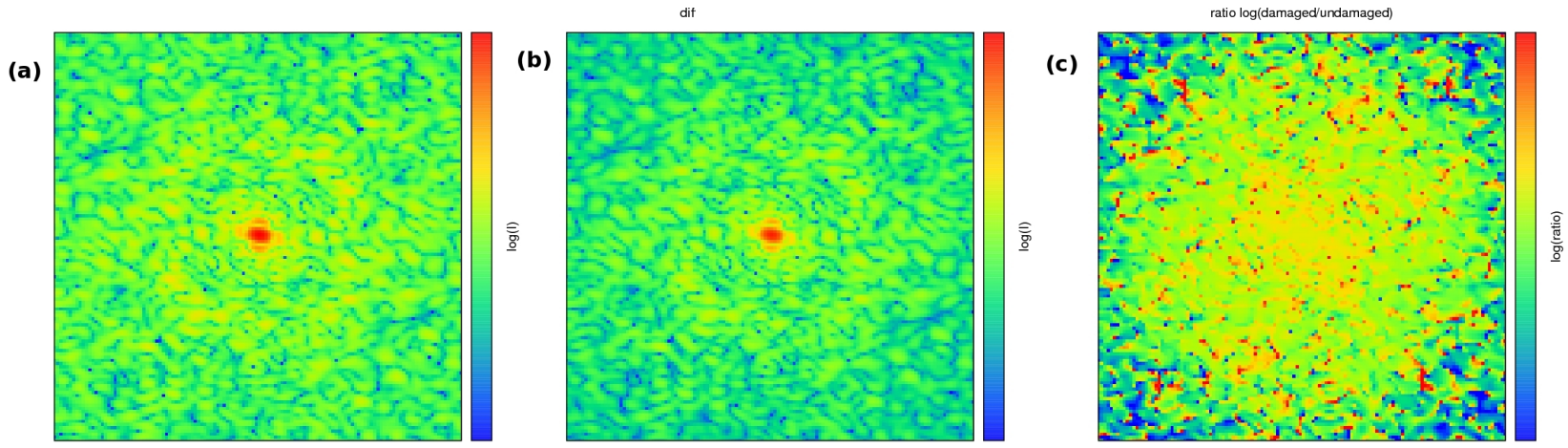

- K-shell depletion reduces the average intensities by a factor of approximately six at the resolution limit (1Å).

- Statistical fluctuations lead to the blurring of the diffraction pattern and the elimination of intensity zeros, hindering reconstruction.

Electrodynamical approach: *Electrodynamical CDI*

The "diffract and destroy" paradigm requires accumulation of data from equivalent molecular orientations, but must also recognize shot-to-shot electronic variations (implications for data orientation).

- There is a smooth decay in intensity at high q due to the *average* depopulation of inner-shell electrons
- The positions of the zeros shift substantially if the degree of damage is large, because of the fluctuations in the individual atomic form-factors.

The second effect can be removed by a simple deconvolution if the damage fraction is less than 25%, so adopt "average atom" model.

Modal dimension reduces from $\simeq e^{2000}$ to about 10, based on quasi-homogeneous approximation in partially-coherent optical theory (Born and Wolf).

Electrodynamical approach: *Electrodynamical CDI*

Taking electrodynamic damage over many frames into account, we have

$$I(\mathbf{q}) = \sum_{ZZ'} A_{ZZ'}(q) T_Z(\mathbf{q}) T^*_{Z'}(\mathbf{q})$$

where

$$\begin{aligned} A_{ZZ'}(q) &= \sum_{\gamma\gamma'} \bar{A}^{Z\gamma,Z'\gamma'} f^{Z\gamma}(q) f^{Z'\gamma'}(q) \\ T_Z(\mathbf{q}) &= \sum_{m_Z} \exp(-i\mathbf{q}\cdot\mathbf{R}^Z_{m_Z}). \end{aligned}$$

The electronic damage, the temporal variation in illumination and the *partially coherent* optical properties are contained in $A_{ZZ'}(q)$ and the required structural information is in $T_Z(\mathbf{q})$ (readily extended to include vibrational factors).

Nuclear density representation

On the assumption that the nuclei don't move throughout the interaction, a fully-coherent quantity is the nuclear density, $T(\mathbf{q})$, where

$$T(\mathbf{q}) = \sum_Z Z T^Z(\mathbf{q}) = \sum_Z Z \sum_{m_Z} \exp(-i\mathbf{q}\cdot\mathbf{R}^Z_{m_Z}).$$

Rather than try and correct $I(\mathbf{q})$ to find $\varrho(\mathbf{r})$, we seek a $q-$dependent transformation that enables us to find $T(\mathbf{q})$

$$I(\mathbf{q}) = T^*(\mathbf{q})B(\mathbf{q})T(\mathbf{q})$$

If the function $B(\mathbf{q})$ can be determined, $I(\mathbf{q})/B(\mathbf{q})$ and *a priori* information define a conventional *single mode* inverse problem for $T(\mathbf{q})$.

Iterative reconstruction of bacteriorhodopsin

Nuclear density, $t(\mathbf{r}) = \mathcal{F}[T(\mathbf{q})]$

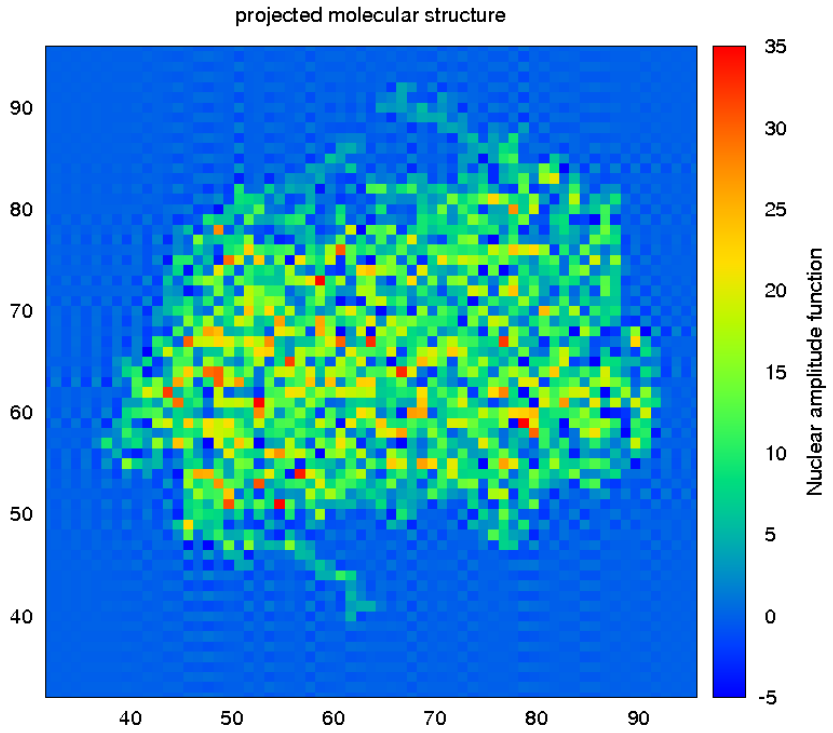

The 'chemical structure' is obtained by interpolation on $t(\mathbf{r})$ to find $\{\mathbf{R}^Z_{m_z}\}$ directly, rather than fitting a density model. Image recovered by HIO iterations with loose support and charge-flipping, followed by error-reduction.

What a seeded XFEL source has to offer

The success of this approach depends *critically* on being able to distinguish between

- the statistical intensity fluctuations of the illumination and
- the statistical fluctuations in the scattering target.

If the statistics of the illumination $\mathcal{I}_n(t)$ are well-characterized *and* well-sampled then a seeded (quasi-monochromatic) XFEL source would make it possible to perform experiments to determine $A_{ZZ'}(q)$ and, if necessary, additional effects that arise due to the high-intensity breakdown of the quasi-homogeneous approximation of partial coherence (Lorenz *et al.*, PRL, submitted 2012). This would remove the reliance on modelling of these electronic effects (Curwood *et al.* PRA, to be submitted 2012).

Determination of $A_{ZZ'}(q)$ from $I(\mathbf{q})$

The function $A_{ZZ'}(q)$ depends on (i) the statistical properties of $\{\mathcal{I}_n(t)\}$ and (ii) the electrodynamics of the constituent atoms (given (i)).

Assume that we possess a molecule of (a) known structure, (b) similar chemical composition and molecular weight relative to unknown sample.

Can then determine $A_{ZZ'}(q)$ from experimental data, $I(\mathbf{q})$; this $A_{ZZ'}(q)$ is transferable to the determination of an unknown structure, $T(\mathbf{q})$, provided that $\{\mathcal{I}_n(t)\}$ possesses the same statistical properties and a sufficiently large sample is obtained.

Ultimately, "the determination of $A_{ZZ'}(q)$" involves the determination of a finite set of real, positive numbers, $\bar{A}^{Z\gamma,Z'\gamma'}$.

A straightforward non-linear optimization scheme correctly determines these parameters, starting with guesses based on undamaged values (Curwood, Nugent and Quiney, 2012).

Disorder in nanocrystalline XFEL imaging of biomolecules

- Many biomolecules only form small (possibly 2D) nanocrystals rather than high-quality crystals for crystallography.
- The reason crystals stop growing is presumed to be surface disorder.
- Disorder will reduce effective coherence of Bragg diffraction, affecting shape of Bragg peaks; assume effect depends on surface to bulk ratio, N_S/N_V.
- If the nanocrystal is sufficiently small and ordered one sees diffraction between Bragg peaks.
- If the nanocrystal is both small and exhibits surface disorder, can one still extract structure using XFEL sources and *continuous*-$\mathbf{q}$ CDI-based methods (avoiding molecular replacement modelling)?

Nanocrystalline imaging of biomolecules with XFEL

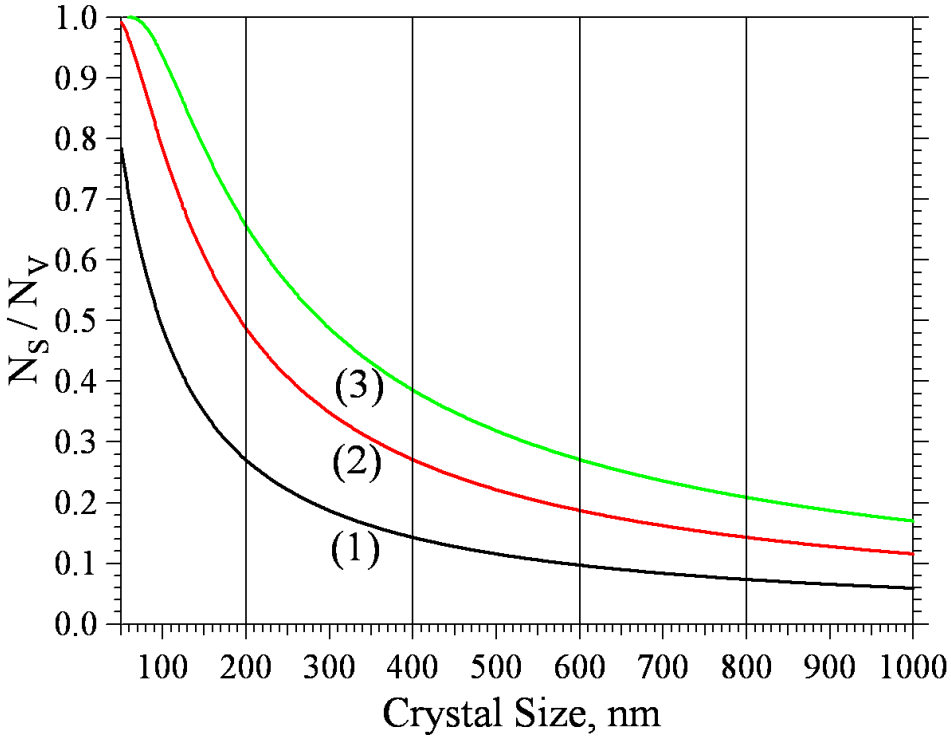

Ratio of surface to bulk molecules, N_S N_V, as a function of crystal size for different unit cell parameters: (1) a = 10.0 nm, (2) a = 20.0 nm, and (3) a = 30.0 nm.

Nanocrystalline imaging of biomolecules with XFEL

Incorporate disorder into nanocrystalline modelling in a manner similar to that employed for electronic damage.

$$I(\mathbf{q}) = |F(\mathbf{q})|^2 \cdot \tilde{\Lambda}(\mathbf{q})$$

$$\tilde{\Lambda}(\mathbf{q}) = \sum_{jk} \exp(i\mathbf{q}\cdot\mathbf{R}_j) g_{jk}(\mathbf{q}) \exp(-i\mathbf{q}\cdot\mathbf{R}_k)$$

where $F(\mathbf{q})$ is the molecular (unit-cell) form-factor, $\tilde{\Lambda}(\mathbf{q})$ is the interference function and the summations are over all unit cells.

The *complex* factor $g_{jk}(\mathbf{q})$ incorporates information about disorder (perfect order restored if $g_{jk}(\mathbf{q}) = 1$, independent of $\mathbf{q}$.

Nanocrystalline imaging of biomolecules with XFEL

Can define two classes of disorder function, g_{jk}:

1: Orientational disorder

$$g_{jk}(\mathbf{q}) = \min\left(\frac{1-(12q^2D_m^2)^{-1}}{qG(\mathbf{q})D_m}, 1\right)$$

2: Positional disorder

$$g_{jk}(\mathbf{q}) = \exp(-2\pi^2 q^2 \Delta_m^2)$$

$m = |j-k|$, D_m is the distance between clusters, $G(\mathbf{q})$ is the 'preferred orientation' function, Δ_m^2 is the mean-square displacement of the m^{th} cluster pair.

Nanocrystalline imaging of biomolecules with XFEL

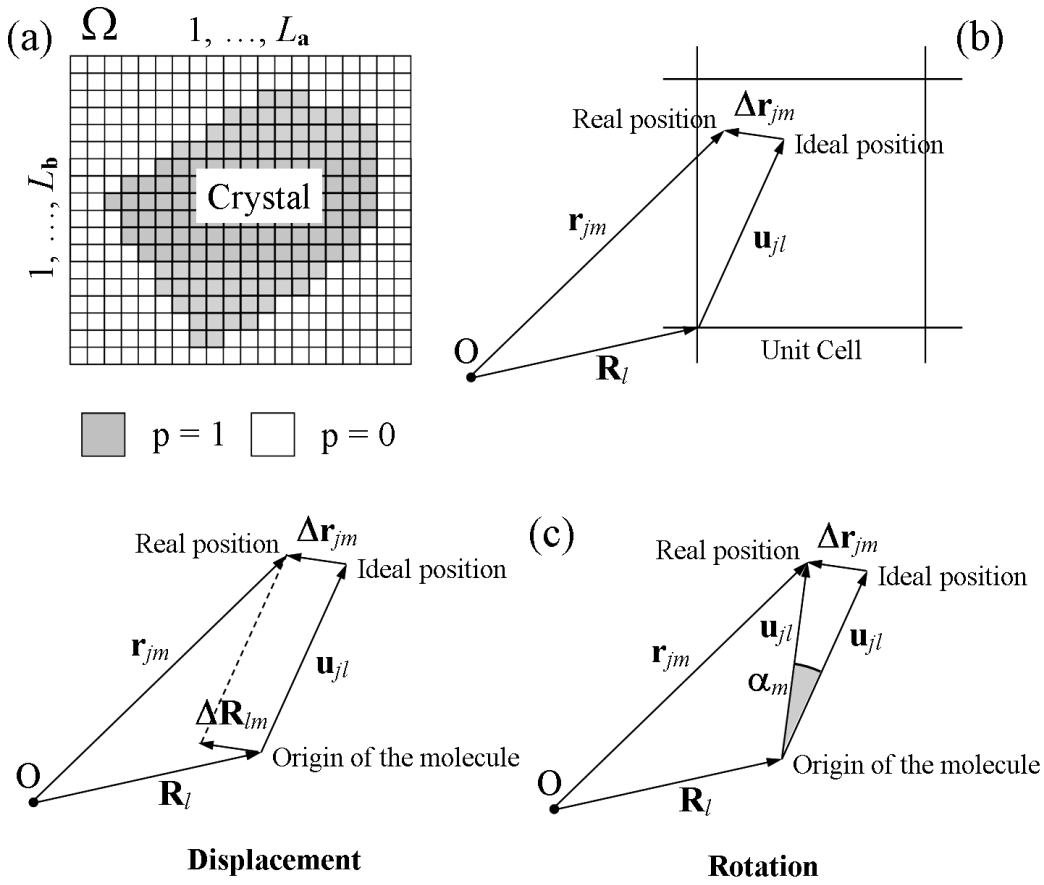

Each partially-ordered nanocrystal defined by site occupancies and local displacements and rotations.

Nanocrystalline imaging of biomolecules with XFEL

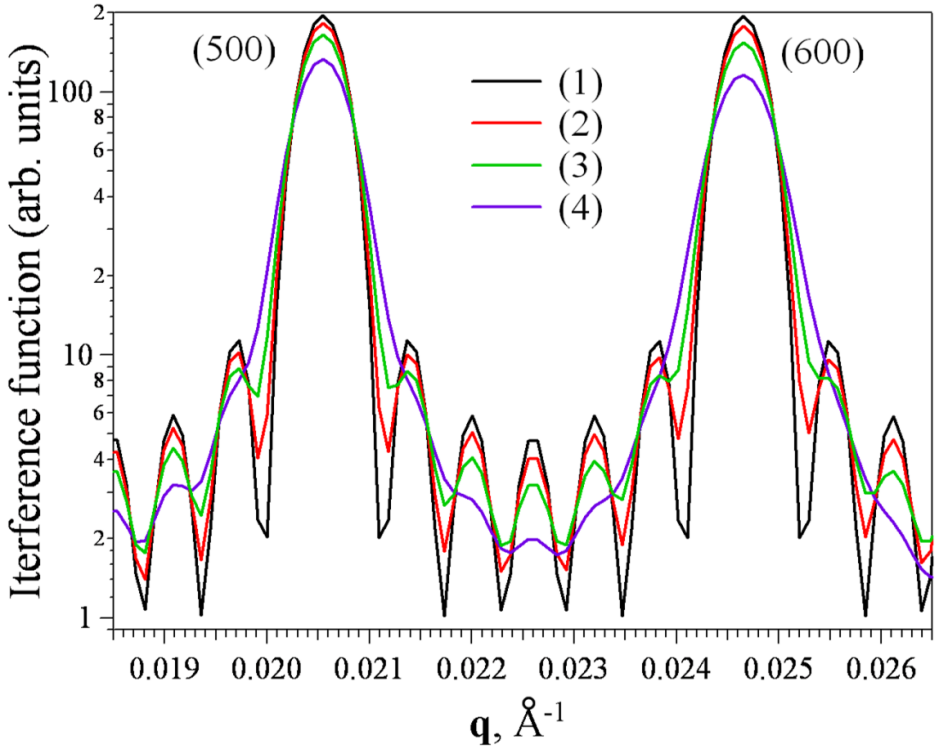

Variation of $\tilde{\Lambda}(\mathbf{q})$ between (500) and (600) Bragg reflections (hexagonal unit cell, a = b = 281 Å, and c = 165 Å). Assumes $\Delta_m^2 = \alpha d_{100}$, where d_{100} is the interplanar distance along the (100) direction of the crystal lattice: (1) α= 0.0, (2) α = 0.002, (3) α= 0.005, and (4) α = 0.008.

Nanocrystalline imaging of biomolecules with XFEL

Just as we found in the case of electronic damage (which imparts electronic disorder on the structure factor), we find that:

$$I(\mathbf{q}) = \sum_{jk} T_j(\mathbf{q}) A_{jk} T_k^*(\mathbf{q})$$

where

$$A_{jk} = \langle p_j p_k \exp(i\mathbf{q}\cdot(\Delta R_j - \Delta R_k)) \rangle$$

The average is taken over the site occupancies and disorder parameters of a collection of nanocrystals.

In this case, the known functions $T_j(\mathbf{q})$ are constructed from the positions of the *perfectly* ordered crystal lattice sites.

The description of disorder is now at the level of site positions and site occupancies rather than at the atomic level.

Nanocrystalline imaging of biomolecules with XFEL

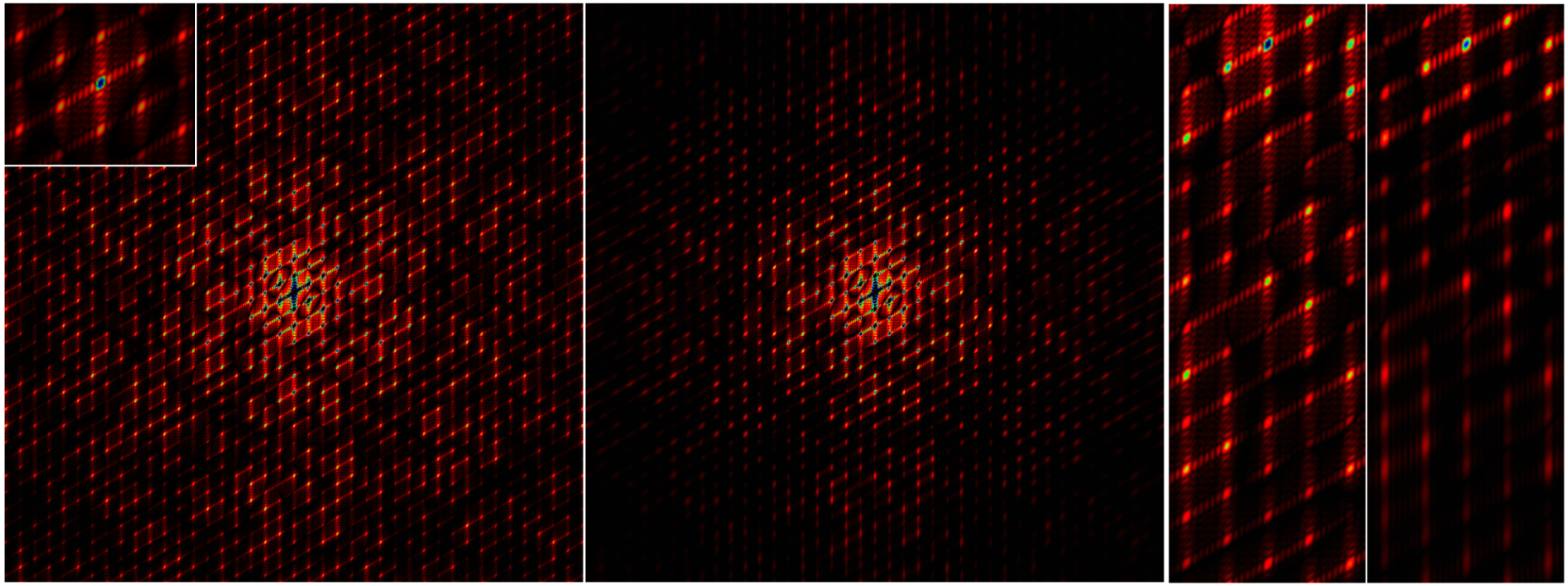

Simulated diffraction patterns of the Photosystem I nanocrystal ((ab) plane): (a) ideal crystal; (b) disordered crystal. (c) A magnified views of ideal (left) and disordered (right) nanocrystal diffraction.

Reconstruction algorithm

The disorder is incorporated in $\mathbf{A}(\mathbf{q})$

$$A_{jk}(\mathbf{q}) = |\langle W(\mathbf{q})\rangle|^2 \otimes g_{jk}(\mathbf{q})$$

where $\langle W(\mathbf{q})\rangle$ is the average crystal shape factor.

$$T_j(\mathbf{q}) = F(\mathbf{q}) \exp(-i\mathbf{q}\cdot\mathbf{R}_j).$$

$F(\mathbf{q})$ initialized with uniform, normalized distribution. Modulus constraint is applied in $\mathbf{q}$-space

$$|T'_j(\mathbf{q})| = |T_j(\mathbf{q})| \sqrt{\frac{I_0}{I_{calc}}}$$

A single mode, $T_0(\mathbf{q})$ (in the bulk) is propagated to real space and the support constraint applied to that unit cell.

Nanocrystalline imaging of biomolecules with XFEL

- Simulate nanocrystals of Photosystem I (mean dimensions 7×7×12 unit cells; ≃200 nm; variable disorder to $R > 100$).

- Two data sets of integrated Bragg intensities for ideal, $I_i(hkl)$, and disordered, $I_d(hkl)$ protein nanocrystals; 2.5 Å resolution.

- Molecular replacement with PHASER (McCoy et al., 2007) using published Photosystem I structure (Protein Data Bank ID, 1JB0) as an initial model for $F_i(hkl) = \sqrt{I_i(hkl)}$ and $F_d(hkl) = \sqrt{I_d(hkl)}$.

- Constrained structural refinement with REFMAC (Murshudov et al., 1997) *failed* to determine a structure from I_d, even with extremely high thermal parameters in the range of 40-120 Å^2

- Reconstruction to 4.1 Å resolution using PCDI (no molecular replacement).

Nanocrystalline imaging of biomolecules with XFEL

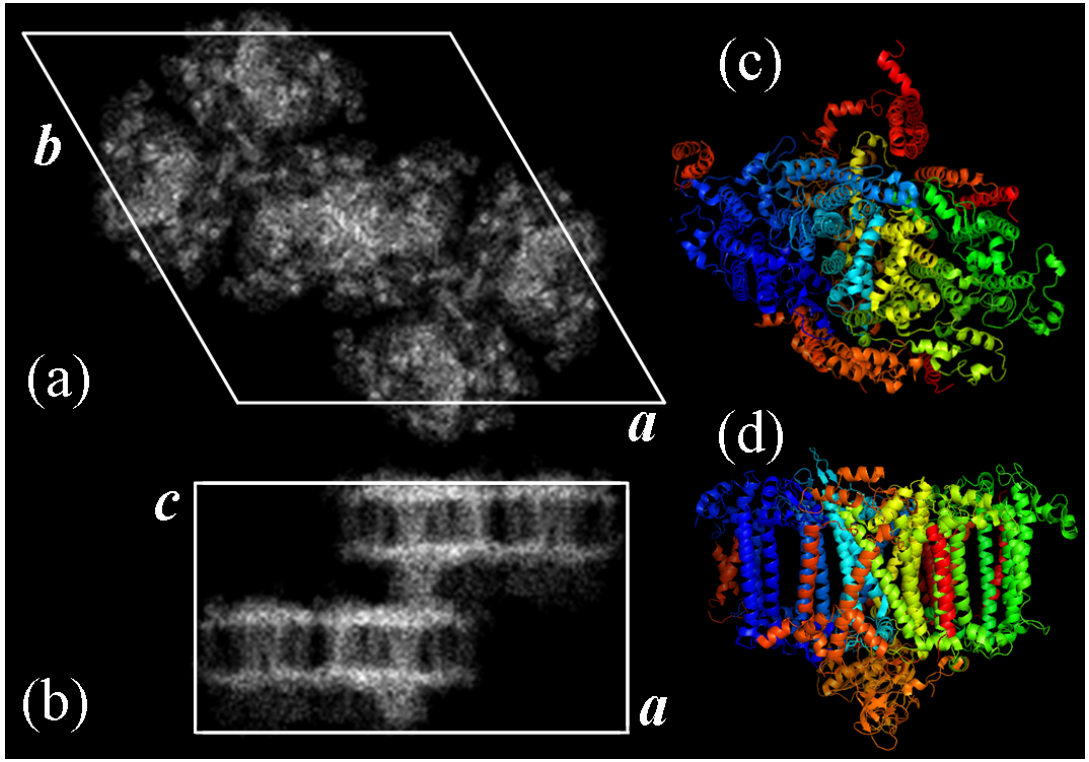

Electron density of the Photosystem I molecular cluster, reconstructed with resolution of 4.1 Å by incorporating models of the partial coherency: (a) (ab) crystallographic plane, (b) (ac) crystallographic plane. (c) and (d) models of the Photosystem I molecule, (ab) and (ac) projections.

New opportunities for molecular imaging with XFEL

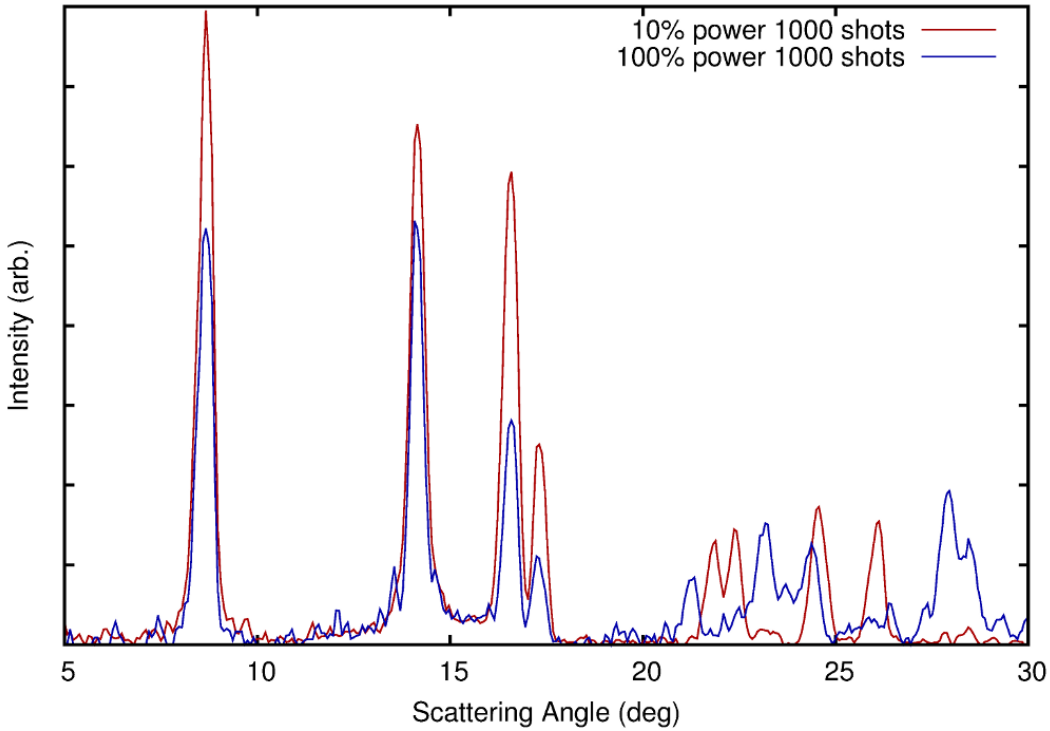

Radially averaged diffraction of C_{60} at 10% power and maximum power (LCLS, 10keV, 30 fs pulses, 100 $(nm)^2$ focus.

New opportunities for molecular imaging with XFEL

Fullerenes and their ions are known to exhibit a range of unusual properties, including orientational phase transitions. At -20 ^{o}C, a phase transition of the FCC room temperature structure begins to a SC structure (0.1 Å lattice parameter change).

In our experiment, we see reflections appear at high intensities that are *forbidden* for FCC structures and features characteristic of FCC that are strongly suppressed at high intensity. The low power pattern is *almost* identical to synchrotron data.

These effects are believed to be driven by an *intramolecular* Jahn-Teller effect and the *pseudorotation* of this vibronic distortion (dynamic JT effect). This pseudorotation time has been estimated variously from picoseconds to femtoseconds.

New opportunities for molecular imaging with XFEL

- This pseudorotation time in C_{60} is apparently of order femtoseconds for inner-shell excitation.

- In the 30 fs duration of our experiment, we see the clear signature of a structural change in C_{60} that only occurs at intensities above some threshold spanned by the limits of our experiment.

- It may well also be further driven by subsequent inner-shell electronic rearrangements that lower the overall energy of the system.

- Determining the precise conditions under which this transition occurs will require more careful control of the intensity of the incident pulses (or at least some diagnostic information).

- Seeded pulses promise *ultimately* to deliver this control.

Conclusions

- Explicit inclusion of partial coherence known to dramatically improve reconstruction quality in X-ray diffractive imaging.
- Electronic damage in biomolecular XFEL imaging generates a partially-coherent scattered wave, even if illumination fully coherent.
- Structural disorder in nanocrystals also carries the signature of a partially coherent scattered wave.
- Ultimately, you can only incorporate or extract statistical information about the scattering target if such information is not overwhelmed by statistical fluctuations in the source.
- The statistical control afforded by seeding is likely to provide its most significant contribution to molecular XFEL imaging.